NEOPLASIA
www.neoplasia.com

Volume 18 Number 3 March 2016 pp. 152–161 152

Rat Prostate Tumor Cells Progress in the Bone Microenvironment to a Highly Aggressive Phenotype[1]

Sofia Halin Bergström, Stina H Rudolfsson and Anders Bergh

Department of Medical Biosciences, Pathology, Umeå University, Umeå, Sweden

Abstract

Prostate cancer generally metastasizes to bone, and most patients have tumor cells in their bone marrow already at diagnosis. Tumor cells at the metastatic site may therefore progress in parallel with those in the primary tumor. Androgen deprivation therapy is often the first-line treatment for clinically detectable prostate cancer bone metastases. Although the treatment is effective, most metastases progress to a castration-resistant and lethal state. To examine metastatic progression in the bone microenvironment, we implanted androgen-sensitive, androgen receptor–positive, and relatively slow-growing Dunning G (G) rat prostate tumor cells into the tibial bone marrow of fully immune-competent Copenhagen rats. We show that tumor establishment in the bone marrow was reduced compared with the prostate, and whereas androgen deprivation did not affect tumor establishment or growth in the bone, this was markedly reduced in the prostate. Moreover, we found that, with time, G tumor cells in the bone microenvironment progress to a more aggressive phenotype with increased growth rate, reduced androgen sensitivity, and increased metastatic capacity. Tumor cells in the bone marrow encounter lower androgen levels and a higher degree of hypoxia than at the primary site, which may cause high selective pressures and eventually contribute to the development of a new and highly aggressive tumor cell phenotype. It is therefore important to specifically study progression in bone metastases. This tumor model could be used to increase our understanding of how tumor cells adapt in the bone microenvironment and may subsequently improve therapy strategies for prostate metastases in bone.

Neoplasia (2016) 18, 152–161

Introduction

Metastasis to bone is one of the most important clinical features of prostate cancer (PC). Approximately 70% of patients have prostate tumor cells in their bone marrow already at diagnosis [1]. Although the existence of such disseminated tumor cells (DTCs) is a predictor of recurrence [1,2], not all of the DTCs grow into clinically detectable metastases [1]. Why only subsets of asymptomatic and dormant micrometastases progress into clinical overt metastases is largely unknown.

Androgen deprivation therapy is a common first-line therapy for metastatic PC. Although the initial response to androgen deprivation is of significant palliative value, the metastases progress into an incurable and fatal state termed *castration-resistant PC*. A better understanding of the biology behind metastatic progression, from dormant asymptomatic micrometastases to clinically detectable metastases and from overt metastases to castration-resistant disease, is therefore a key to development of more effective treatments for metastatic PC.

The ability to grow as a clinically detectable metastasis could be acquired in the primary tumor [3–5]. It is also possible that neoplastic cells that are able to survive in the bone microenvironment progress at

Abbreviations: PC, prostate cancer; DTCs, disseminated tumor cells; BrdU, bromodeoxyuridine; DHT, dihydrotestosterone; T, testosterone; FBS, fetal bovine serum; AR, androgen receptor; CSC, cancer stem cells.

Address all correspondence to: Sofia Halin Bergström, Department of Medical Biosciences, Pathology, 6M, Second floor, Umeå University, SE-90185, Umeå, Sweden.
E-mail: sofia.halin@umu.se

[1] This work was supported by grants from the Swedish Research Council (grant number Co257301), the Swedish Cancer Foundation (grant number 130293), Lion's Cancer Research Foundation at Umeå University, and the Queen Viktorias Freemason Foundation.
Received 3 November 2015; Revised 21 January 2016; Accepted 25 January 2016

1476-5586
http://dx.doi.org/10.1016/j.neo.2016.01.007

the metastatic site in parallel with those in the primary tumor, regarding both intrinsic properties of the neoplastic cells and development of a metastasis stroma [3–5]. The prognosis may therefore depend on the ability of the initially dormant metastatic cells to grow and interact with the different microenvironment at the metastatic site.

PC cells have been shown to home to the hematopoietic stem cell niche in bone and replace the hematopoietic stem cells, and this niche appears to support tumor dormancy [6]. The formation of both osteolytic and osteoblastic lesions at the metastatic site in bone suggests that interactions with the microenvironment are crucial for the establishment of bone metastases [7]. Moreover, both adaptive and innate immunity may control the establishment of metastases. Low levels of the histocompatibility leukocyte antigen class I molecule on breast cancer cells have been suggested to be a way for DTCs to escape from T-cell–induced cytotoxicity and subsequently facilitate metastatic outgrowth [8]. The activity of T-cells may also be suppressed in the bone microenvironment in PC [9]. Better *in vivo* models that enable studies of metastatic progression in the factual microenvironment of fully immune-competent animals are therefore needed. Furthermore, bone marrow DTCs from breast, prostate, and esophageal cancer have been shown to display significantly fewer genetic aberrations than primary tumor cells [10–13], suggesting that they are disseminated early during primary tumor progression. Cell lines from more advanced metastatic tumors may therefore not be useful in studies of metastatic progression, as the mechanisms that are crucial for early colonization and adaptive selection may have been altered. Furthermore, neoplastic cells continue to evolve genetically at the bone metastatic site, and metastasis-to-prostate and metastasis-to-metastasis spread has been shown to be common in PC patients [14,15].

Here we implanted androgen-sensitive, androgen receptor (AR)–positive, and relatively slow-growing and poorly metastatic Dunning G (G) rat prostate tumor cells [16] into the tibial bone marrow of fully immune-competent Copenhagen rats. The aim of this study was to develop an *in vivo* model that reflects several aspects of human PC bone metastases and to determine whether the bone microenvironment can induce stable changes in prostate tumor cells, primarily regarding growth rate, the ability to colonize secondary organs, and response to androgen deprivation.

Materials and Methods

Cell Culture and Animals

Androgen-sensitive, AR-positive, low-metastatic rat prostate G R3327 tumor cells were grown in RPMI 1640 + GlutaMAX (Gibco) supplemented with 10% fetal bovine serum (FBS) and 250 nM dexamethasone [16]. Adult syngenic and fully immune-competent male Copenhagen rats (Charles River, bred in our laboratory) were used in all animal experiments. All the animal work was carried out in accordance with protocols approved by the Umeå Ethical Committee for Animal Studies (permit number A110-12).

Intraprostatic and Intratibial Implantation of G Prostate Tumor Cells

For intraprostatic implantation simulating primary tumor growth, the animals were anesthetized, and an incision was made in the lower abdomen to expose the ventral prostate lobes. G tumor cells were carefully injected into one of the ventral prostate lobes using a Hamilton syringe. For intratibial injections simulating metastatic growth, the animals were anesthetized, and the right leg of the rat was flexed. Using a drilling motion, a 23G needle was inserted via the knee joint into the bone marrow cavity of the tibia, and G tumor cells were then injected directly into the bone marrow cavity.

The same number of G tumor cells (2×10^5 cells in 10 µl of RPMI) was implanted into the prostate or bone marrow as described above, and the animals were sacrificed 8 weeks later (n = 10 rats with prostate tumors, n = 10 rats with bone tumors) and 12 weeks later (n = 6 rats with prostate tumors, n = 6 rats with bone tumors). The prostatic tumors were removed and fixed in formalin for 24 hours, dehydrated, and paraffin embedded. The right leg was cut above the knee and formalin fixed for 48 hours, decalcified in formic acid–sodium citrate solution (30% and 15%, respectively) for 48 hours, dehydrated, and embedded in paraffin.

Castration Treatment

Rats were castrated by scrotal incision or they were sham operated (control) 7 days before implantation of tumor cells. G tumor cells (2×10^6) were implanted into the ventral prostate of castrated rats (n = 9) or control rats (n = 8). In separate animals, G tumor cells were implanted into the bone marrow of both tibias (2×10^6/tibia) in castrated rats (n = 5) and control rats (n = 6) as described above. All animals were sacrificed 6 weeks after implantation of tumor cells, and 1 hour before sacrifice, the animals were injected with bromodeoxyuridine (BrdU, 50 mg/kg; Sigma-Aldrich), and the tumors were removed and formalin fixed as described above.

In addition, G tumor cells were implanted into the ventral prostate (2×10^3 cells) and the tibial bone marrow (2×10^5 cells) of the same animals. After 8 weeks, the animals were randomized to receive sham (n = 7) or castration treatment (n = 8). The animals were injected with BrdU as described above and sacrificed 14 days after the treatment was started.

To label hypoxic cells, additional animals that had been castrated (n = 6) or sham operated (n = 5) for 7 days were injected with Hypoxyprobe (Millipore) 1 hour before sacrifice, and the prostates, livers, kidneys, and tibial bones were formalin fixed and embedded in paraffin as described earlier [17]. Tissue oxygen was also measured directly in the bone marrow and prostate in anesthetized rats using electrodes (LIcox, Mediplast, Malmö, Sweden, probe CC1.2) inserted in the same way as for intratibial or intraprostatic tumor cell injection.

To measure dihydrotestosterone (DHT) and testosterone (T), animals that had been castrated (n = 7) or sham operated (n = 7) for 7 days were sacrificed, and the ventral prostate lobes and the tibias and femurs were immediately frozen in liquid nitrogen. In addition, EDTA plasma was collected. DHT and T were measured in bone marrow, prostate tissue, and plasma (at the Swedish Metabolomics Centre, Umeå, Sweden) using liquid chromatography–tandem mass spectrometry as previously described [18].

Morphological Analysis

Tumor area was assessed in hematoxylin and eosin–stained sections using Pannoramic viewer software version 1.15 (3DHistech, www.3dhistech.com). For G tumors in the prostate, the largest tumor area of each tumor represented tumor size. In bone, the G tumors usually grew as multiple tumors within the bone marrow cavity and sometimes also in the joint cavity. Representative bone sections were analyzed, and the section with the largest total tumor area (the sum of all G tumor areas present) in each animal was chosen to represent tumor size in bone. Sections were immunostained using

primary antibodies against BrdU (Dako), caspase-3 (Cell Signaling Technology), and Hypoxyprobe (Chemicon) as previously described [17]. To determine proliferation (BrdU) and apoptosis (caspase-3), the fractions (i.e., percentages) of stained cells were assessed in approximately 1000 cells.

Reestablishment of G Tumor Cells In Vitro

Rats were castrated or sham operated 7 days before intratibial implantation of 2×10^5 G tumor cells. After 8 and 12 weeks, the tumors were reestablished as tumor cell lines *in vitro* as previously described [16]. Briefly, bone marrow containing the tumor cells was excised aseptically, minced with scissors, and mixed with 10 ml of 0.1% collagenase in Hanks' balanced salt solution (HBSS) containing calcium and magnesium (Gibco) and incubated in 37°C for 1 hour. The mixture was filtered through a 100-μm cell strainer (BD Falcon). The first filtrate was discarded, the residue was washed on the cell strainer with calcium- and magnesium-free HBSS (Gibco), and the wash was discarded. The cells were gently pressed through the strainer and washed with 20 ml of HBSS. The cells that passed through the filter were centrifuged (500*g* for 5 min) and resuspended in complete medium. Cells from each tumor group were pooled as one cell line (n = 5 to 6 tumors/cell line) and incubated at 37°C, 5% CO_2.

Western Blot

Protein was extracted from the reestablished G tumor cell lines as previously described [19]. Equal amounts of total cell lysates were separated on a 10% TGX gel under reduced conditions (Bio-Rad, Sundbyberg, Sweden), blotted onto a nitrocellulose membrane using the Trans-Blot Turbo transfer system (Bio-Rad), and incubated overnight at 4°C with an anti-AR antibody (PG-21; Upstate) and an anti–β-actin antibody (A2066; Sigma-Aldrich). Following incubation with primary antibodies and washing, the membranes were incubated with species-appropriate IRDye secondary antibodies (800CW and 680RD; LI-COR Biosciences, Cambridge, UK) for 1 hour at room temperature. The membranes were analyzed using the Odyssey CLx system (LI-COR), and relevant signal intensity was determined using LI-COR imaging software.

3-(4,5-Dimethylthiazol-2-yl)-2,5diphenyltetrazolium Bromide (MTT) Viability Assay

Viability was determined with the MTT assay (Roche Diagnostics). Briefly, G tumor cells from bone (5×10^3 cells/well, 6 wells/cell line and time point) were seeded in 100 μl of complete medium in 96-well plates and incubated in 37°C for 1 to 7 days. After each time point, 10 μl of MTT labeling agent was added to each well and incubated for an additionally 4 hours. Then, 100 μl of solubilization solution was added to each well, with incubation overnight. The absorbance was measured at 550 nm the following day and subtracted with the reference wavelength at 650 nm.

For DHT and T stimulation, tumor cells were seeded in phenol red–free (androgen-free) RPMI 1640 (Gibco) with 2.5% charcoal-stripped (androgen-free) FBS (Gibco) in 96-well plates and incubated in 37°C (5×10^3 cells/well, 6 wells/concentration and time point). After 24 hours, the cells were incubated with indicated concentrations of DHT, T, or vehicle for 7 days, and the absorbance was measured as described above.

Reinjection of Reestablished G Cells in Rat Prostate, Bone, and Lungs

The reestablished cells were cultured for 5 to 8 passages (to reduce stromal contamination), and then 2×10^5 cells from each cell line (G-original, G-bone-8w, G-bone-8w-cast, G-bone-12w, and G-bone-12w-cast) were reinjected into the ventral prostate of new recipient rats that had been castrated or sham treated 1 week earlier as described above (n = 5 to 6 in each group). After six weeks, the animals were sacrificed, and the tumors were removed, weighed, and formalin fixed. The G-bone-12w tumor cells were also reinjected into the bone marrow and prostate (2×10^5 cells/site, n = 7), and tumors were formalin fixed after 4 weeks. Original G tumor cells and the different sublines of G tumor cells reestablished from bone (7.5×10^5 cells in 0.3 ml of RPMI, n = 5 to 7 animals/cell type) were also injected into the rat tail vein, and 10 weeks later, the lungs were removed, weighed, and formalin fixed.

Statistical Analysis

Mann-Whitney U test and Kruskal-Wallis H test (both nonparametric) were used for comparisons between groups. Any P value $< .05$ was considered significant. Statistical analysis was performed using the statistical software SPSS version 22.0. Values presented are mean ± SE.

Results

Establishment of G Tumors in Bone and Prostate

To examine the establishment and growth of prostate tumor in the bone, we implanted androgen-sensitive G rat prostate tumor cells (2×10^5 cells) into the tibial bone marrow of fully immune-competent Copenhagen rats. At 8 weeks, small tumor foci (resembling micrometastases) were found in the bone marrow (Figure 1*A*). At 12 weeks, the tumors were 3 times larger than at 8 weeks and occupied substantial parts of the bone marrow cavity (macrometastases), and they had sometimes grown outside the bone or into the knee joint (Figure 1, *A* and *B*).

In addition, we implanted an equal number of G tumor cells in the prostate to determine whether tumor establishment in the prostate (i.e., the primary site) was different from that in the bone microenvironment (i.e., the metastatic site). In the prostate, each rat developed a single spherical tumor which, by 8 weeks, had invaded the whole prostate (Figure 1*A*). At 12 weeks, the tumors were twice as large as they had been 4 weeks earlier (Figure 1*B*). The tumors established in the prostate were, however, 31 times larger at 8 weeks and 23 times larger at 12 weeks than the tumors established in bone (Figure 1*B*), suggesting that, at least initially, the bone microenvironment was of poorer quality for the tumor cells than the prostate microenvironment.

Establishment of G Tumors in the Bone Microenvironment of Castrated Rats

G tumors are not dependent on androgen for their survival, but their growth rate is reduced when they grow subcutaneously in castrated rats and mice [20,21].

To study how low androgen levels affected G tumor establishment in the bone microenvironment, we implanted G tumor cells into the tibial bone marrow of rats that had been castrated or sham operated 1 week earlier. As tumor establishment was slow in bone, we injected 10 times the number of cells described above (2×10^6) and evaluated tumor size after 6 weeks. At this time point, there was no significant difference between G tumors in the bone of control rats and castrated rats (Figure 2*A*), indicating that androgen deprivation did not affect tumor establishment in bone.

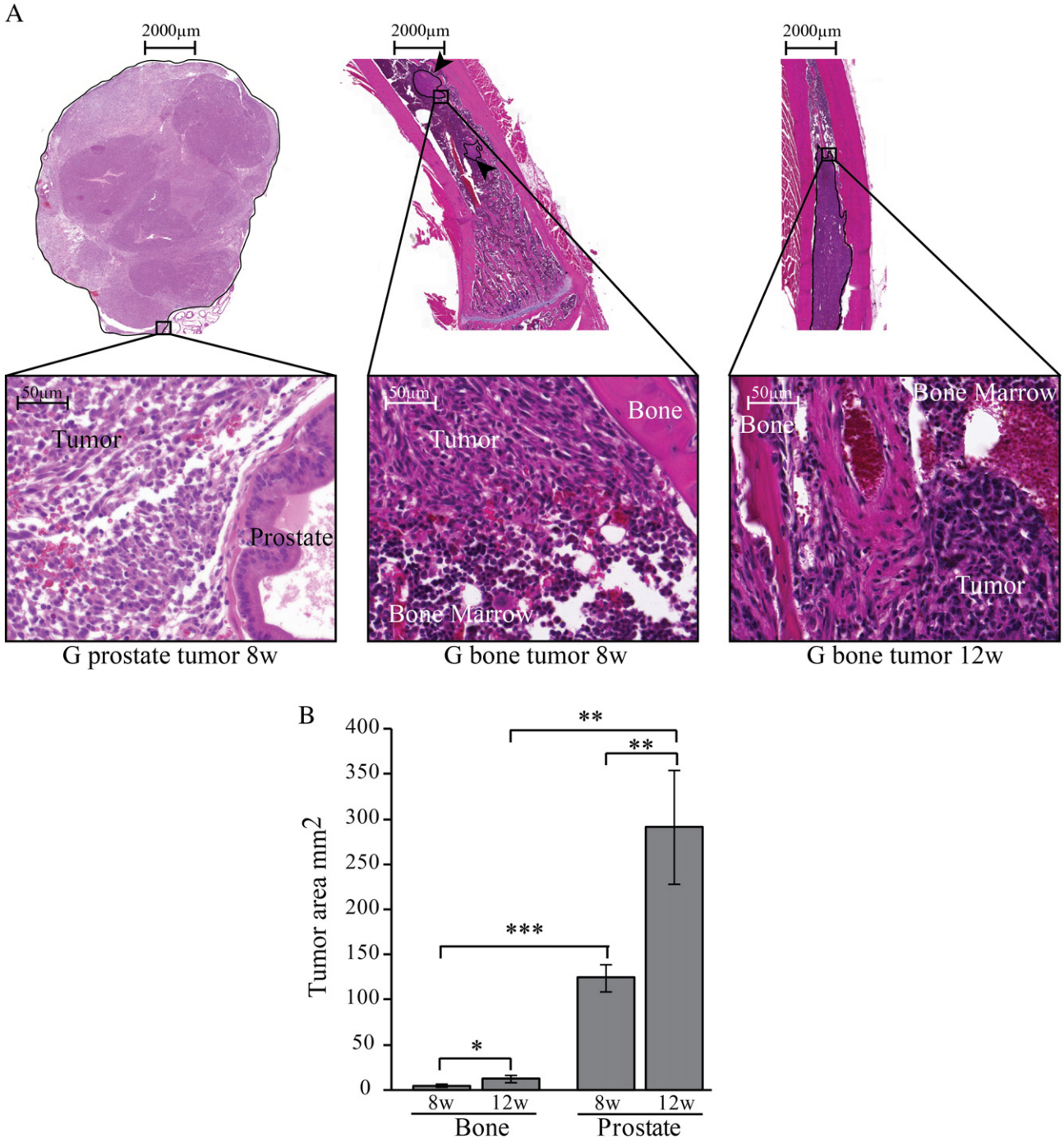

Figure 1. Establishment of G tumors in the bone versus the prostate microenvironment. G tumor cells (2×10^5) were implanted into the tibial bone marrow or ventral prostate of fully immune-competent rats. (A) Representative sections, in low and high magnifications, of G tumors in prostate at 8 weeks (encircled in black) and in bone at 8 weeks (encircled in black and with arrowheads) and 12 weeks (encircled in black). High-resolution versions of G tumors in prostate and bone slides for use with the Virtual Microscope are available as eSlide: VM02511 and as eSlide: VM02512. (B) Tumor area (mm^2) in bone and prostate at 8 and 12 weeks. Values are mean ± SE; $n = 6$ to 10 animals in each group. *$P < .05$, **$P < .01$, ***$P < .001$.

As a control, the same number of cells was injected into the prostate of castrated or sham-operated rats, and tumor size was evaluated 6 weeks later. Again, the tumors in control rats were significantly larger in the prostate than in bone (Figure 2*A*). G tumor size in the prostate was, however, significantly reduced (by 95%) in castrated rats, whereas no such reduction was seen in the bone. Tumor proliferation (BrdU-labeling index) was similar in control tumors in bone and prostate, showing that tumor growth was similar at the end of the experiment. This suggests that tumor growth was comparable in the prostate and bone once the tumors were established. At 6 weeks, proliferation was significantly reduced at both sites in castrated compared with control rats (Figure 2*B*).

Castration Treatment of Established G Tumors in the Bone Microenvironment

In the clinical setting, androgen deprivation is initiated when patients already have advanced local or metastatic PC. We therefore

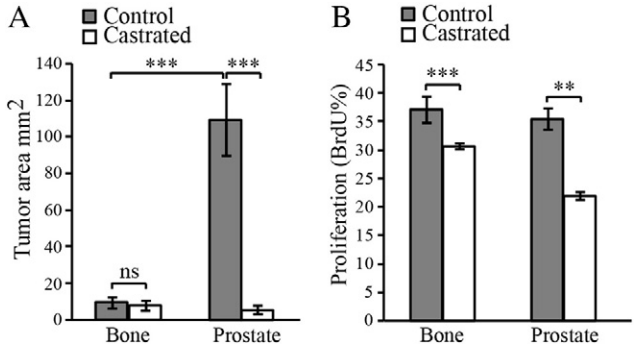

Figure 2. Tumor establishment in bone and prostate of castrated and control rats. G tumor cells (2×10^6) were implanted into the tibial bone marrow or prostate tissue of control or castrated rats, and tumor size (A) and tumor proliferation (BrdU) (B) were analyzed at 6 weeks. Values are mean ± SE, $n = 8$ to 12 animals in each group, $^{**}P < .01$, $^{***}P < .001$, ns = not significant.

evaluated how already established tumors in bone and prostate responded to castration. G tumor cells were implanted into the prostate and bone marrow of the same animals. To somewhat compensate for the slower tumor establishment in bone, we injected 100-fold more cells in the bone marrow (2×10^5) than in the prostate (2×10^3). After 8 weeks, the animals were randomized to receive either castration or control treatment, and the tumors were analyzed 14 days later. G tumors in the prostate of castrated rats were 83% smaller than prostate tumors in control animals, whereas G tumor size in bone was apparently unaffected by castration (Figure 3*A*). Proliferation and apoptosis were unaffected by castration in the tumors in bone (Figure 3, *B* and *C*). In contrast, proliferation was significantly decreased and apoptosis significantly increased by castration in the tumors in prostate (Figure 3, *B* and *C*). This shows that the response to castration is reduced for G tumors growing in bone compared with G tumors established in the prostate.

G Tumor Progression in the Bone Microenvironment

To further determine whether G tumor cells progress and change their phenotype over time in the bone microenvironment, i.e., whether they gradually become more aggressive and/or castration resistant, G cells were again implanted into the tibial bone marrow of rats that had been castrated or sham operated 1 week earlier (Figure 4*A*). After tumor establishment, the G tumors were removed, pooled, and reestablished as the following cell lines *in vitro* (Figure 4*A*): 1) G cells from microscopic 8-week bone tumors of control animals (G-bone-8w), 2) G cells from 8-week bone tumors of castrated rats (G-bone-8w-cast), 3) G cells from macroscopic 12-week bone tumors of control animals (G-bone-12w), and 4) G cells from 12-week bone tumors of castrated rats (G-bone-12w-cast).

No apparent difference was seen in the cell morphology between the reestablished cell lines *in vitro,* and they were morphologically similar to that of the original G cells (Figure 4*B*). The reestablished tumor cells were cultured *in vitro* for several passages to reduce possible contamination by stromal cells. In the bone-derived cell lines, the gene expressions of mesenchymal markers and epithelial cell markers did not indicate an enrichment of mesenchymal cells compared with the original G cell line (unpublished observations from whole genome expression array). G-bone-12w cells and G-bone-12w-cast cells had higher viability *in vitro* than the G-original, G-bone-8w, and G-bone-8w-cast tumors cells (Figure 4*C*), indicating that G tumor cells from macroscopic bone tumors had become more aggressive. Using Western blot, we observed that all the different G cell lines expressed the AR with slightly lower levels in G-bone-8w-cast cells and G-bone-12w-cast cells (Figure 4*D*). A single band of the AR suggested that there were no AR variants present (Figure 4*D*). In addition, nuclear AR levels were also equal in the different cell types, suggesting that all the cell lines still had the same amount of AR signaling (data not shown).

To compare the growth rates and androgen sensitivities of the different bone-derived G tumor cell lines *in vivo*, we reinjected an equal number of cells from each cell line into the prostate of new recipient rats that had been castrated and control treated 1 week earlier, and then analyzed the tumors 6 weeks later (Figure 5, *A* and *C*). G-bone-8w and G-bone-8w-cast tumor cells gave slightly larger tumors than the G-original cells when reinjected into the prostate, and both cell types responded to castration with reduced tumor size compared with controls (Figure 5*A*), suggesting that early and microscopic G prostate tumors in bone had only somewhat progressed. Interestingly, G-bone-12w and G-bone-12w-cast tumor cells were highly aggressive when reinjected into the prostate (Figure 5*A*). G-bone-12w tumor cells

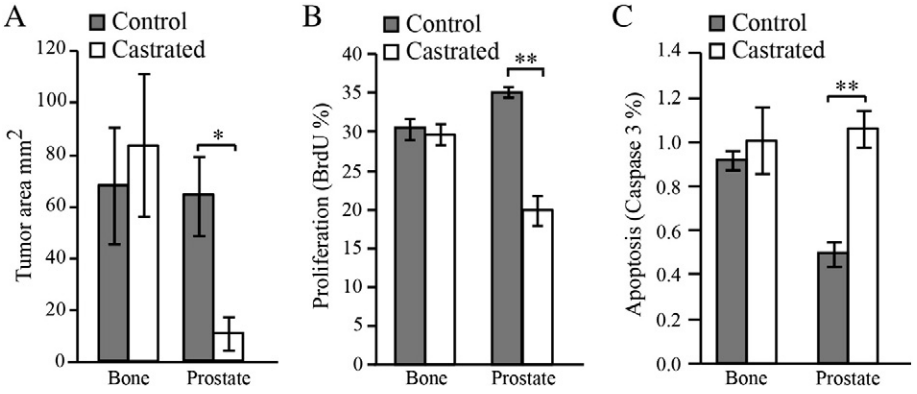

Figure 3. Castration treatment of established G tumors in the bone microenvironment. G tumor cells were implanted into the bone marrow (2×10^5) and into the prostate tissue (2×10^3) and grown for 8 weeks, and then the rats were either castrated or control treated. Tumor size (A), tumor proliferation (BrdU) (B), and tumor apoptosis (caspase-3) (C) were analyzed 14 days later. Values are mean ± SE; $n = 7$ to 8 animals in each group. $^{*}P < .05$, $^{**}P < .01$.

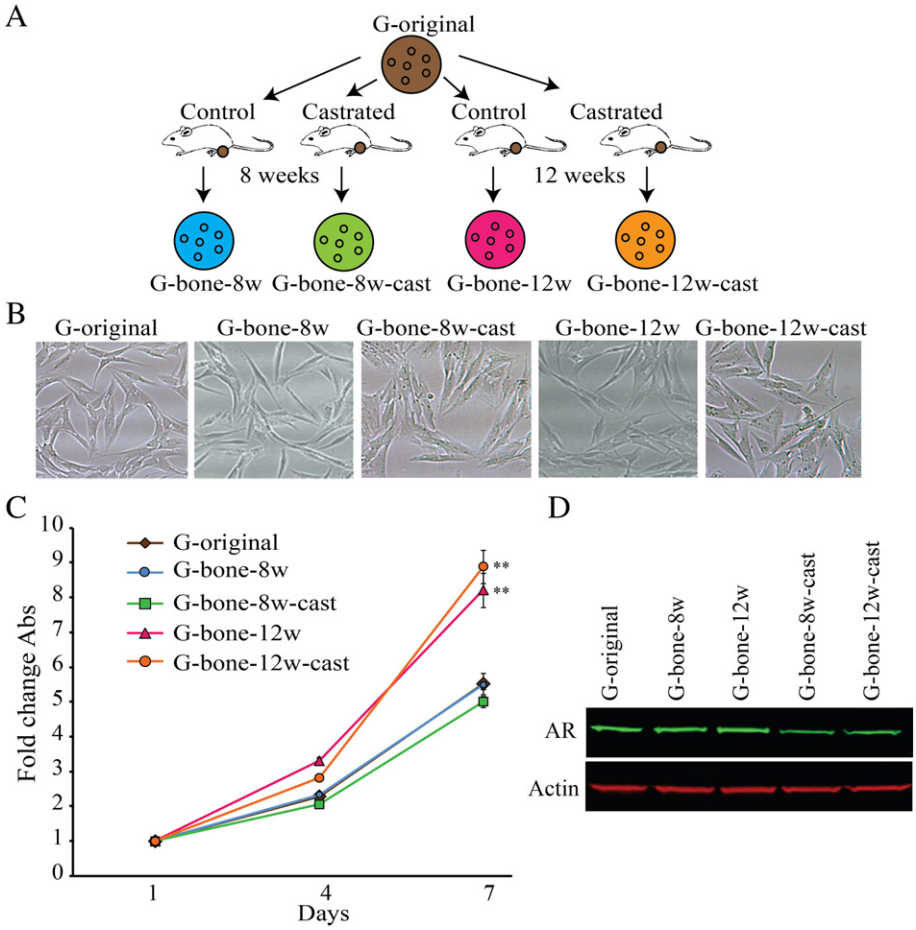

Figure 4. G tumor progression in the bone microenvironment. (A) G tumor cells (2×10^5) were injected into the tibial bone marrow of castrated or control-treated rats and left for 8 or 12 weeks before tumors ($n = 5$ to 6 in each group) were removed, pooled, and reestablished *in vitro* as the following cell lines: G cells from 8-week bone tumors of control animals (G-bone-8w), G cells from 8-week bone tumors of castrated rats (G-bone-8w-cast), G cells from 12-week bone tumors of control animals (G-bone-12w), and G cells from 12-week bone tumors of castrated rats (G-bone-12w-cast). (B) Tumor cell morphology *in vitro* was similar to that of the original G cells. (C) Tumor cell viability measured for 7 days *in vitro* using an MTT assay, presented as fold change in mean absorbance (abs) ± SE compared with day 1. $^{**}P < .01$ compared with the original G cell line at day 7. (D) Western blot analyses showing androgen receptor levels in the different G tumor cell lines.

formed tumors in the prostate that were 18 times larger than the original G tumors, and although the G-bone-12w tumors still responded to castration, the magnitude of the response was less (tumor size in castrated tumors was 62% of that in the controls) than in the original tumors (11% of controls), the G-bone-8w tumors (8% of controls), and the G-bone-8w-cast tumors (24% of controls) (Figure 5*A*). Reinjection of G-bone-12w-cast tumor cells into the prostate resulted in the largest tumors (28 times larger than the original G tumors), which were also totally castration resistant (Figure 5*A*). In addition, the G-bone-12-w-cast tumors differed in morphology from the other tumor types, with large abnormal blood vessels with viable tumor tissue immediately around each vessel, whereas areas further away from the vessels were necrotic (Figure 5*C*). This suggests that, with time, the G tumors in the bone microenvironment progress to an aggressive phenotype. Interestingly, the G-bone-12w tumor cells had reduced androgen sensitivity *in vivo,* which would suggest that the bone microenvironment *per se* could promote castration resistance.

Next, we examined establishment of the aggressive G tumor cells in bone. G-bone-12w tumor cells (2×10^5) were injected into both the tibial bone marrow and the prostate, and tumor size was evaluated after 4 weeks. As early as 4 weeks, the G-bone-12w tumors were established in the bone in 7 out of 7 animals, with a similar mean tumor area (3.58 ± 1.79 mm^2, $n = 7$) to that of the original G tumors at 8 weeks (Figure 1*B*), suggesting that the tumor cells had adapted to grow in the bone microenvironment. However, the G-bone-12w tumor cells were still significantly smaller in the bone than in the prostate (mean tumor area 29.85 ± 4.31 mm^2, $n = 7$;+$P = .002$), indicating that the bone microenvironment also suppressed the growth of more aggressive tumors.

None of the G tumor cell lines that were reinjected into the prostate were spontaneously metastasizing (data not shown). To examine tumor colonization and growth in the lungs, the different G bone tumor cells from bone were injected into the tail vein of rats. Both the G-bone-12w tumors and the G-bone-12w-cast tumors had taken over most of the lung tissue by 10 weeks, and the experiment had to be terminated (Figure 5, *B* and *D*). At this time point, we could only find small tumors in the lungs of animals injected with the G-original, the G-bone-8w, and the G-bone-8w-cast tumor cells (Figure 5, *B* and *D*).

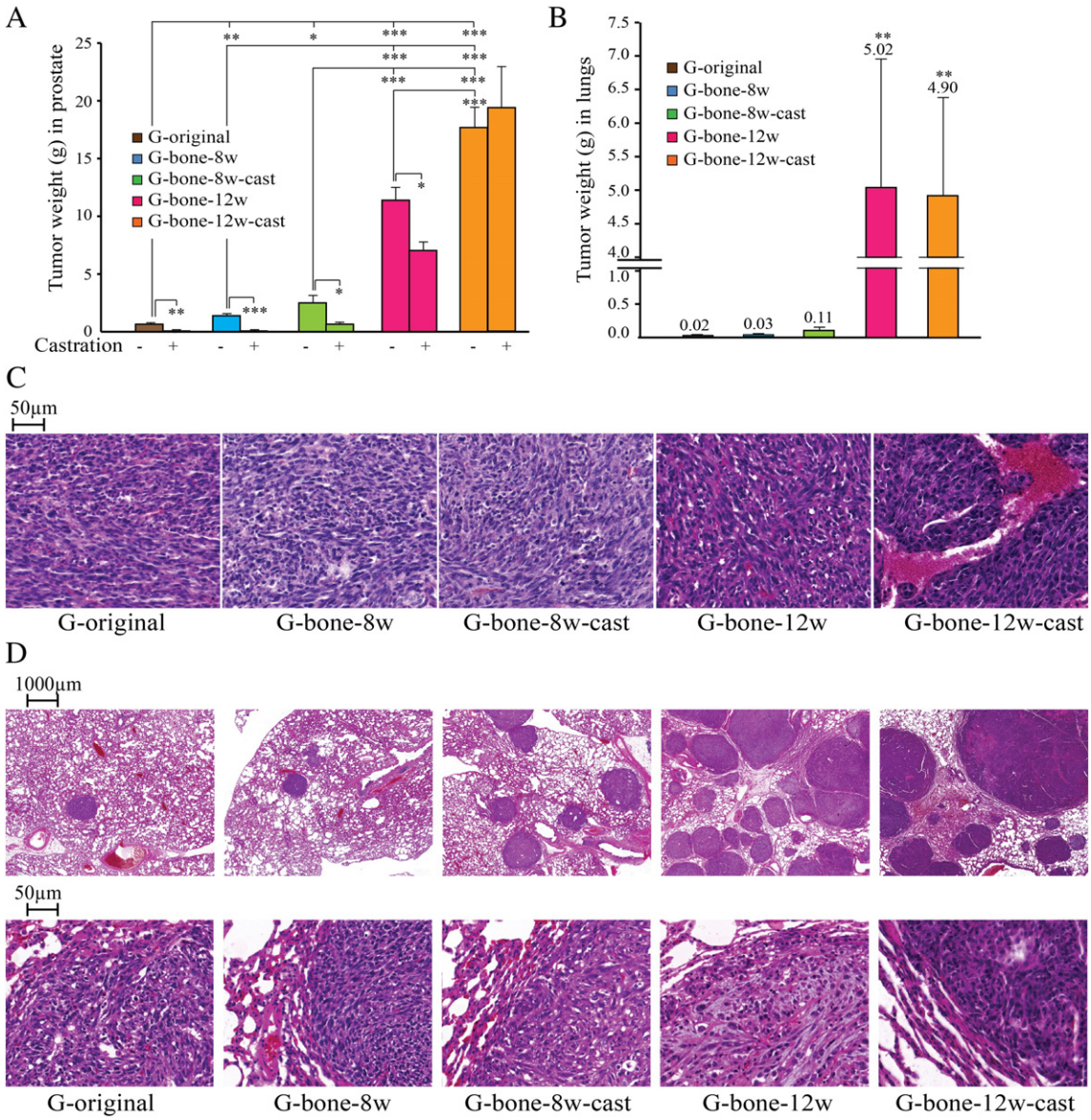

Figure 5. G tumor progression in the bone microenvironment. (A) Equal numbers (2×10^5 cells) from the different G tumor cell lines were reinjected into the ventral prostate of recipient rats that had been castrated or control treated, and tumor weight was measured 6 weeks later (values are mean ± SE, $n = 6$ to 8 in each group; $^*P < .05$, $^{**}P < .01$, $^{***}P < .001$). (B) Equal numbers of cells of each G cell line (7.5×10^5) were injected into the tail vein, and tumor colonization in lungs was examined 10 weeks later (values are mean tumor weight in lungs ± SE, $n = 5$ to 7 in each group, $^{**}P < .01$ compared with G-original cells). (C) Sections of the different G tumors in prostate. Note the changed morphology in the G-bone-cast-12w tumors, with viable tumor tissue growing around large blood vessels. High-resolution versions of G-bone-8w-cast and G-bone-12w-cast slides for use with the Virtual Microscope are available as eSlide: VM02513 and as eSlide: VM02514. (D) Representative sections, in low and high magnifications, showing lung tumor burden for the different cell lines. High-resolution versions of G-bone-8w and G-bone-12w slides for use with the Virtual Microscope are available as eSlide: VM02515 and as eSlide: VM02516.

Lung tumor burden was significantly higher in animals injected with either G-bone-12w cells or G-bone-12w-cast cells compared with the other three cell types (Figure 5*B*). Our results show that G tumor cells that had progressed in the bone microenvironment had an increased capacity to colonize secondary organs, such as the lungs. Tumor cells growing in bone could therefore be a source of a subsequent (i.e., secondary) wave of metastatic dissemination to other tissues or back to the prostate [14,15].

Taken together, the difference between tumor cells from microscopic 8-week and macroscopic 12-week G prostate bone tumors showed that new tumor cell characteristics, resulting in more aggressive tumor cells with reduced androgen sensitivity, were stably acquired with time in the bone microenvironment.

Concentrations of Testosterone and Dihydrotestosterone in the Normal Prostate and Bone

Slow initial growth and the subsequent development of an aggressive tumor cell phenotype in the bone could be due to microenvironmental factors. Using liquid chromatography–tandem mass spectrometry [18], we therefore compared the local levels of T and DHT in prostate tissue and bone marrow of tumor-free control rats and tumor-free castrated rats. In the prostate tissue, the

concentration of DHT was high (Table 1) and in similarity with previous reports [22]. Although T signals were detected in prostate tissue of untreated rats, the levels were below the quantification limit (Table 1). This indicates that T is rapidly converted to DHT in the prostate. The bone marrow did not contain measurable DHT, and the concentration of T was six times lower than the intraprostatic levels of DHT (Table 1). In castrated rats, the amount of T was below the limit of detection in both prostate and bone marrow, and the amount of DHT was highly reduced or absent in the prostate (Table 1). T and DHT were also measured in plasma, and the concentrations were similar to those previously reported for male rats [22] (Table 1). This shows a difference in both the type and the levels of androgens in prostate tissue and bone marrow.

To study how androgens directly affect G tumor growth and if there was a difference between T and DHT, the cells were stimulated with different concentrations of DHT and T *in vitro*, and tumor cell viability was measured using an MTT assay. The G tumor cells were able to survive for 7 days without any androgens but ceased growing (Figure 6). Both DHT and T were equally effective in stimulating the growth of G tumor cell *in vitro* (Figure 6). This suggests that differences in tumor establishment in bone and prostate *in vivo* are probably not due to variations in the types of androgens. Furthermore, both types of androgens affected tumor cell growth in a dose-dependent manner (Figure 6). The higher levels of androgens in prostate tissue *in vivo* than in the levels in bone marrow may therefore, hypothetically, enhance tumor cell growth in the prostate relative to tumor cell growth in bone.

Hypoxic Conditions in G Tumors in the Bone Marrow and Prostate

Recent studies have shown that bone marrow is highly hypoxic under normal conditions [23]. Hypoxia is known to both suppress tumor growth and drive tumor progression [24]. Using oxygen electrodes and hypoxyprobe staining, we therefore examined the extent of tissue hypoxia in the prostate and bone marrow at the time of tumor cell injection in both castrated rats and control rats.

Hypoxyprobe staining of the tibial bone marrow of untreated rats showed intense staining along the surface of the bone and in scattered islands of hematopoietic cells in the interior of the bone marrow cavity (Figure 7). It was also possible to find areas without staining. The mean oxygen tension (pO_2) was 12.2 ± 1.8 mm Hg (n = 18) in the tibial bone marrow cavity. Seven days after castration, the bone marrow still had intense hypoxyprobe staining, indicating a strong degree of hypoxia (Figure 7), and the mean pO_2 was 8.3 ± 1.2 mm Hg (n = 19). Our previous studies show that castration rapidly reduce prostate blood flow [25] and this results in hypoxia [26,27]. Oxygen levels return to normal levels by day 7 possibly because of low consumption in atrophic glands [26]. In line with this, most of the atrophic prostate glands were unstained at day 7 after castration (data not shown) and as described earlier [26,27]. The mean pO_2 in control prostates (27.2 ± 1.3 mm Hg, n = 13) was significantly higher than in the bone marrow ($P < .001$). We were, however, unable to measure pO_2 in the small prostate remaining at day 7 after castration.

Table 1. Androgen Concentrations in Prostate and Bone Marrow of Tumor-Free Rats

	Testosterone (T) (pmol/g Tissue) (pmol/ml Plasma)		Dihydrotestosterone (DHT) (pmol/g Tissue) (pmol/ml Plasma)	
	Control	Castrated	Control	Castrated
Prostate	<0.12*	0	17.8 ± 3.6	0.06 ± 0.09
Bone marrow	2.9 ± 1.3	0	0	0
Plasma	5.9 ± 2.4	0	1.0 ± 0.9	0

Values are mean ± SD, n = 7 in each group.
*Corresponds to the lowest concentration on the calibration curve.

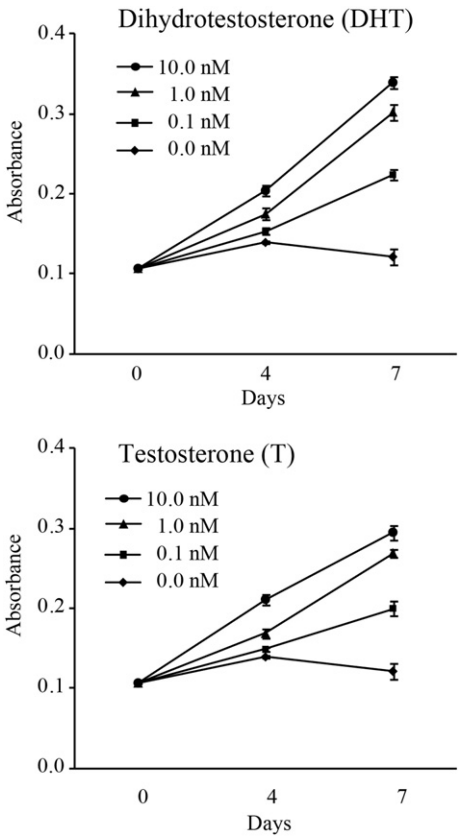

Figure 6. G tumor cell viability in response to androgens. G tumor cell viability *in vitro* was measured 0, 4, and 7 days after incubation with DHT or T at different concentrations using an MTT assay. Values are mean absorbance ± SE.

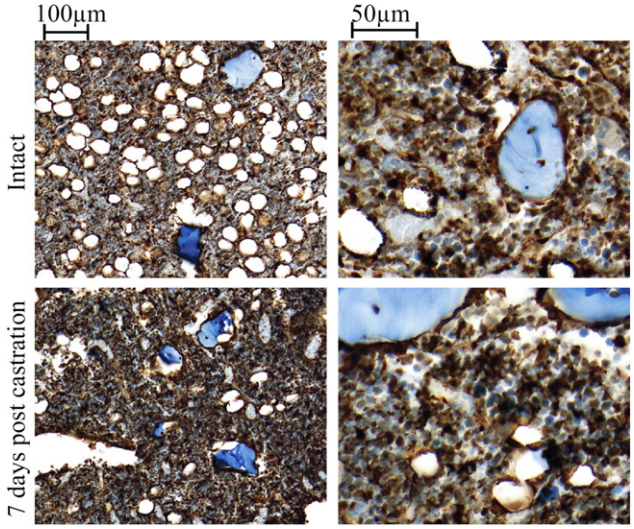

Figure 7. Hypoxia in the bone marrow and prostate. Sections from bone tissue in controls and 7 days after castration, stained for hypoxia (Hypoxyprobe, brown), in low and high magnifications. A high-resolution version of this slide for use with the Virtual Microscope is available as eSlide: VM02517.

Taken together, these results show that G tumor cells implanted in bone need to adapt to a more hypoxic environment than that in the prostate, and this might possibly contribute to the reduced initial tumor growth but also to a stronger selective pressure at the bone metastatic site.

Discussion

To understand the metastatic progression within the bone microenvironment is probably the key to improve treatments for PC metastases. Here we developed an androgen-sensitive rat prostate tumor model and simulated metastases in the bone of fully immune-competent rats. This is an advantage to many other metastasis models that use already castration-resistant tumor cells in immune-compromised animals. We show that G tumor cells reestablished from overt metastases in bone (12 weeks) of both castrated rats and control rats were highly aggressive, with increased ability to grow in prostate, bone, and lungs, in comparison to G tumor cells reestablished from small tumors in bone (8 weeks) and in comparison to the original G tumor cells. Along with this, PC bone metastases in patients seed new metastasis and also reseed back to the prostate [14,15]. Interestingly, dormant breast cancer cells from the bone marrow were highly aggressive when injected at the primary site [28], suggesting that the more aggressive phenotype induced within the bone may show its full potential when the cells arrive at a new site. It appears that slow-growing PC cells within the bone may, with time, acquire traits that facilitate their growth if they reseed the prostate or spread to other secondary sites. This hypothesis is line with the parallel progression model [3], suggesting that early disseminated tumor cells surviving at secondary sites progress differently than those remaining in the primary tumor. Our experimental model can be used to explore the microenvironmental factors in the bone that could be important for metastatic progression and secondary PC metastatic spread.

Furthermore, G tumor cells reestablished from 12-week bone metastases of control rats had reduced androgen sensitivity in the prostate compared with the original G cells, suggesting that the bone microenvironment *per se* promotes castration resistance. Not surprisingly, tumor cells from 12-week bone metastases in castrated rats were totally castration resistant. However, G tumor cells from 8-week bone metastases in both control rats and castrated rats were still androgen sensitive, suggesting that environment-induced castration resistance may need some time to develop. PCs progress in response to androgen deprivation [29], and mutations promoting castration resistance seem to occur after metastatic spread [14]. The mechanisms behind bone-induced versus treatment-induced castration resistance and progression in our model are, at present, unknown. However, up to five serial passages of subcutaneous G tumors in castrated rats did not cause progression of the tumor cells [30], suggesting that the bone microenvironment specifically accelerates prostate tumor progression. We are currently exploring gene expression and genetic and epigenetic profiles of the different G tumor cells from bone to reveal possible novel mechanisms or if mechanisms for castration resistance already shown to be of importance in patients [31] are involved. The possibility that a few cells from the bone microenvironment, such as mesenchymal stem cells [32], may actually survive in the reestablished cell lines and be of functional importance when the cells are injected back into the prostate is also investigated.

Castration treatment before the arrival of tumor cells did not affect G tumor establishment in bone, perhaps suggesting that early androgen deprivation may not affect metastatic colonization in bone. Furthermore, established G tumors in bone did not respond to castration treatment, whereas castration markedly reduced growth of established tumors in the prostate. In line with this, treatment with the antiandrogen bicalutamide reduced tumor growth of a PC xenograft transplanted subcutaneously but not when the same tumor was transplanted into the bone [33]. It appears that the response to castration treatment could be microenvironment dependent. If so, this is of considerable clinical importance.

In this study, we started to explore potential factors in the bone microenvironment that could be involved in the reduced response to castration, the slow initial growth, and the selection of aggressive cancer cells. Here we show that androgen levels are lower in bone than in prostate and that the bone marrow is hypoxic. Whether local androgen levels affect metastatic establishment and progression is unknown and warrants further studies. Hypoxia may induce dormancy in PC metastases [34], suggesting that hypoxia may initiate a more quiescent tumor cell phenotype. Hypoxia may also select for more androgen-independent prostate tumor cells and promote an aggressive tumor cell phenotype [24,35–37]. The reduced response to castration in bone could be due to lack of factors needed for a full castration response. Castration-induced inhibition of primary prostate tumor growth is the result of several factors acting together: direct effects of androgen shortage in epithelial cells, reduced trophic influence from the androgen-dependent prostate stroma, and reduced prostate blood flow causing hypoxia-induced epithelial cell death [17,38–40]. The bone marrow is highly hypoxic already under normal conditions [23], and hypoxia did not appear to increase by castration. Increased hypoxia-induced cell death, as a result of castration, is therefore not likely in the bone environment, and it is unclear whether the bone metastasis stroma and vasculature are as androgen dependent as those in the prostate [41].

In conclusion, using this rat prostate tumor model, we have shown that tumor cells growing in the bone marrow experience lower androgen levels and a higher degree of hypoxia compared with those in the prostate. Importantly, the tumor cells that do survive in the inhospitable microenvironment of bone adapt with time and become much more aggressive and castration resistant. Further studies are therefore needed to detect and treat metastases early before they have progressed and to find mechanisms contributing to the metastatic progression. This tumor model represents different stages of metastatic disease, and it can be used to study processes and mechanisms that are important in metastatic growth and progression to find novel therapeutic targets for bone metastases.

Acknowledgements

We thank Sigrid Kilter, Pernilla Andersson, Susanne Gidlund, and Birgitta Ekblom for skillful technical assistance.

References

[1] Morgan TM, Lange PH, Porter MP, Lin DW, Ellis WJ, Gallaher IS, and Vessella RL (2009). Disseminated tumor cells in prostate cancer patients after radical prostatectomy and without evidence of disease predicts biochemical recurrence. *Clin Cancer Res* **15**, 677–683.

[2] Lilleby W, Stensvold A, Mills IG, and Nesland JM (2013). Disseminated tumor cells and their prognostic significance in nonmetastatic prostate cancer patients. *Int J Cancer* **133**, 149–155.

[3] Klein CA (2009). Parallel progression of primary tumours and metastases. *Nat Rev Cancer* **9**, 302–312.

[4] Quail DF and Joyce JA (2013). Microenvironmental regulation of tumor progression and metastasis. *Nat Med* **19**, 1423–1437.

[5] Sleeman JP (2012). The metastatic niche and stromal progression. *Cancer Metastasis Rev* **31**, 429–440.

[6] Shiozawa Y, Pedersen EA, Havens AM, Jung Y, Mishra A, Joseph J, Kim JK, Patel LR, Ying C, and Ziegler AM, et al (2011). Human prostate cancer metastases target the hematopoietic stem cell niche to establish footholds in mouse bone marrow. *J Clin Invest* **121**, 1298–1312.

[7] Logothetis CJ and Lin SH (2005). Osteoblasts in prostate cancer metastasis to bone. *Nat Rev Cancer* **5**, 21–28.

[8] Pantel K, Schlimok G, Kutter D, Schaller G, Genz T, Wiebecke B, Backmann R, Funke I, and Riethmuller G (1991). Frequent down-regulation of major histocompatibility class I antigen expression on individual micrometastatic carcinoma cells. *Cancer Res* **51**, 4712–4715.

[9] Huen NY, Pang AL, Tucker JA, Lee TL, Vergati M, Jochems C, Intrivici C, Cereda V, Chan WY, and Rennert OM, et al (2013). Up-regulation of proliferative and migratory genes in regulatory T cells from patients with metastatic castration-resistant prostate cancer. *Int J Cancer* **133**, 373–382.

[10] Schardt JA, Meyer M, Hartmann CH, Schubert F, Schmidt-Kittler O, Fuhrmann C, Polzer B, Petronio M, Eils R, and Klein CA (2005). Genomic analysis of single cytokeratin-positive cells from bone marrow reveals early mutational events in breast cancer. *Cancer Cell* **8**, 227–239.

[11] Schmidt-Kittler O, Ragg T, Daskalakis A, Granzow M, Ahr A, Blankenstein TJ, Kaufmann M, Diebold J, Arnholdt H, and Muller P, et al (2003). From latent disseminated cells to overt metastasis: genetic analysis of systemic breast cancer progression. *Proc Natl Acad Sci U S A* **100**, 7737–7742.

[12] Stoecklein NH, Hosch SB, Bezler M, Stern F, Hartmann CH, Vay C, Siegmund A, Scheunemann P, Schurr P, and Knoefel WT, et al (2008). Direct genetic analysis of single disseminated cancer cells for prediction of outcome and therapy selection in esophageal cancer. *Cancer Cell* **13**, 441–453.

[13] Weckermann D, Polzer B, Ragg T, Blana A, Schlimok G, Arnholdt H, Bertz S, Harzmann R, and Klein CA (2009). Perioperative activation of disseminated tumor cells in bone marrow of patients with prostate cancer. *J Clin Oncol* **27**, 1549–1556.

[14] Gundem G, Van Loo P, Kremeyer B, Alexandrov LB, Tubio JM, Papaemmanuil E, Brewer DS, Kallio HM, Hognas G, and Annala M, et al (2015). The evolutionary history of lethal metastatic prostate cancer. *Nature* **520**, 353–357.

[15] Hong MK, Macintyre G, Wedge DC, Van Loo P, Patel K, Lunke S, Alexandrov LB, Sloggett C, Cmero M, and Marass F, et al (2015). Tracking the origins and drivers of subclonal metastatic expansion in prostate cancer. *Nat Commun* **6**, 6605. http://dx.doi.org/10.1038/ncomms7605.

[16] Isaacs JT, Isaacs WB, Feitz WF, and Scheres J (1986). Establishment and characterization of seven Dunning rat prostatic cancer cell lines and their use in developing methods for predicting metastatic abilities of prostatic cancers. *Prostate* **9**, 261–281.

[17] Halin S, Hammarsten P, Wikstrom P, and Bergh A (2007). Androgen-insensitive prostate cancer cells transiently respond to castration treatment when growing in an androgen-dependent prostate environment. *Prostate* **67**, 370–377.

[18] Surowiec I, Koc M, Antti H, Wikstrom P, and Moritz T (2011). LC-MS/MS profiling for detection of endogenous steroids and prostaglandins in tissue samples. *J Sep Sci* **34**, 2650–2658.

[19] Halin S, Wikstrom P, Rudolfsson SH, Stattin P, Doll JA, Crawford SE, and Bergh A (2004). Decreased pigment epithelium-derived factor is associated with metastatic phenotype in human and rat prostate tumors. *Cancer Res* **64**, 5664–5671.

[20] Isaacs JT (1982). Hormonally responsive versus unresponsive progression of prostatic cancer to antiandrogen therapy as studied with the Dunning R-3327-AT and -G rat adenocarcinomas. *Cancer Res* **42**, 5010–5014.

[21] Gao J, Arnold JT, and Isaacs JT (2001). Conversion from a paracrine to an autocrine mechanism of androgen-stimulated growth during malignant transformation of prostatic epithelial cells. *Cancer Res* **61**, 5038–5044.

[22] Kashiwagi B, Shibata Y, Ono Y, Suzuki R, Honma S, and Suzuki K (2005). Changes in testosterone and dihydrotestosterone levels in male rat accessory sex organs, serum, and seminal fluid after castration: establishment of a new highly sensitive simultaneous androgen measurement method. *J Androl* **26**, 586–591.

[23] Spencer JA, Ferraro F, Roussakis E, Klein A, Wu J, Runnels JM, Zaher W, Mortensen LJ, Alt C, and Turcotte R, et al (2014). Direct measurement of local oxygen concentration in the bone marrow of live animals. *Nature* **508**, 269–273.

[24] Rudolfsson SH and Bergh A (2009). Hypoxia drives prostate tumour progression and impairs the effectiveness of therapy, but can also promote cell death and serve as a therapeutic target. *Expert Opin Ther Targets* **13**, 219–225.

[25] Lekas E, Johansson M, Widmark A, Bergh A, and Damber JE (1997). Decrement of blood flow precedes the involution of the ventral prostate in the rat after castration. *Urol Res* **25**, 309–314.

[26] Rudolfsson SH and Bergh A (2008). Testosterone-stimulated growth of the rat prostate may be driven by tissue hypoxia and hypoxia-inducible factor-1alpha. *J Endocrinol* **196**, 11–19.

[27] Shabsigh A, Ghafar MA, de la Taille A, Burchardt M, Kaplan SA, Anastasiadis AG, and Buttyan R (2001). Biomarker analysis demonstrates a hypoxic environment in the castrated rat ventral prostate gland. *J Cell Biochem* **81**, 437–444.

[28] Marsden CG, Wright MJ, Carrier L, Moroz K, and Rowan BG (2012). Disseminated breast cancer cells acquire a highly malignant and aggressive metastatic phenotype during metastatic latency in the bone. *PLoS One* **7**, e47587.

[29] Karantanos T, Corn PG, and Thompson TC (2013). Prostate cancer progression after androgen deprivation therapy: mechanisms of castrate resistance and novel therapeutic approaches. *Oncogene* **32**, 5501–5511.

[30] Humphries JE and Isaacs JT (1982). Unusual androgen sensitivity of the androgen-independent Dunning R-3327-G rat prostatic adenocarcinoma: androgen effect on tumor cell loss. *Cancer Res* **42**, 3148–3156.

[31] Watson PA, Arora VK, and Sawyers CL (2015). Emerging mechanisms of resistance to androgen receptor inhibitors in prostate cancer. *Nat Rev Cancer* **15**, 701–711.

[32] Jung Y, Kim JK, Shiozawa Y, Wang J, Mishra A, Joseph J, Berry JE, McGee S, Lee E, and Sun H, et al (2013). Recruitment of mesenchymal stem cells into prostate tumours promotes metastasis. *Nat Commun* **4**, 1795.

[33] Godebu E, Muldong M, Strasner A, Wu CN, Park SC, Woo JR, Ma W, Liss MA, Hirata T, and Raheem O, et al (2014). PCSD1, a new patient-derived model of bone metastatic prostate cancer, is castrate-resistant in the bone-niche. *J Transl Med* **12**, 275.

[34] Mishra A, Wang J, Shiozawa Y, McGee S, Kim J, Jung Y, Joseph J, Berry JE, Havens A, and Pienta KJ, et al (2012). Hypoxia stabilizes GAS6/Axl signaling in metastatic prostate cancer. *Mol Cancer Res* **10**, 703–712.

[35] Ghafar MA, Anastasiadis AG, Chen MW, Burchardt M, Olsson LE, Xie H, Benson MC, and Buttyan R (2003). Acute hypoxia increases the aggressive characteristics and survival properties of prostate cancer cells. *Prostate* **54**, 58–67.

[36] Butterworth KT, McCarthy HO, Devlin A, Ming L, Robson T, McKeown SR, and Worthington J (2008). Hypoxia selects for androgen independent LNCaP cells with a more malignant geno- and phenotype. *Int J Cancer* **123**, 760–768.

[37] Alqawi O, Wang HP, Espiritu M, and Singh G (2007). Chronic hypoxia promotes an aggressive phenotype in rat prostate cancer cells. *Free Radic Res* **41**, 788–797.

[38] Franco OE and Hayward SW (2012). Targeting the tumor stroma as a novel therapeutic approach for prostate cancer. *Adv Pharmacol* **65**, 267–313.

[39] Lissbrant IF, Lissbrant E, Damber JE, and Bergh A (2001). Blood vessels are regulators of growth, diagnostic markers and therapeutic targets in prostate cancer. *Scand J Urol Nephrol* **35**, 437–452.

[40] Johansson A, Jones J, Pietras K, Kilter S, Skytt A, Rudolfsson SH, and Bergh A (2007). A stroma targeted therapy enhances castration effects in a transplantable rat prostate cancer model. *Prostate* **67**, 1664–1676.

[41] Crnalic S, Hornberg E, Wikstrom P, Lerner UH, Tieva A, Svensson O, Widmark A, and Bergh A (2010). Nuclear androgen receptor staining in bone metastases is related to a poor outcome in prostate cancer patients. *Endocr Relat Cancer* **17**, 885–895.